We are IntechOpen, the world's leading publisher of Open Access books

Built by scientists, for scientists

6,900
Open access books available

185,000
International authors and editors

200M
Downloads

Our authors are among the

154
Countries delivered to

TOP 1%
most cited scientists

12.2%
Contributors from top 500 universities

BOOK CITATION INDEX
CLARIVATE ANALYTICS
INDEXED

WEB OF SCIENCE™

Selection of our books indexed in the Book Citation Index
in Web of Science™ Core Collection (BKCI)

Interested in publishing with us?
Contact book.department@intechopen.com

Analysis of Heat Transfer in an Experimental Heat Exchanger Using Numerical Simulation

Laura L. Castro, Alfredo Aranda and
Gustavo Urquiza

Additional information is available at the end of the chapter

Abstract

In this chapter, an analysis of convection heat transfer in an experimental heat exchanger using experimental data and numerical simulation data (by means **computational fluid dynamics** (CFD)) is presented. Work was realized in four stages. In the first stage, experimental data were obtained from a heat exchanger installed in Thermohydraulic Laboratory from CIICAp. Analytic calculus with experimental data was realized in the second stage to establish proper values in boundary and operation conditions for numerical simulation. The third stage includes numerical simulation using CFD of the heat exchanger domain with both working fluids (air-water). At the fourth stage, an analysis of the results was performed.

The obtained results are a fair representation of theoretical behavior since phenomena such as thermal and hydrodynamic boundary layers can be observed, which are in function of the flow, either laminar or turbulent. The production of vortices in the case of air in the area of wake is also observed, all this information is useful for optimization and to propose other arrangements that are to be studied in order to achieve improvements in efficiency of heat exchanger. The averaged errors between analytical calculus estimated using experimental data and numerical simulations did not exceed 20%. The ratio between simulation and real heat exchange is 85%.

Keywords: Heat Exchanger, Heat Transfer, computational fluid dynamics, CFD

1. Introduction

Analysis of heat transfer is necessary for optimization and better use of energy resources of the heat exchangers; we provide the necessary information in terms of the behavior of fluids in

certain areas or arrangements to which more heat is transferred so that the more information about the process is known; it will be possible to have a device with lower maintenance costs or energy supply. Currently, computational fluid dynamics (CFD) has been emerged as a powerful tool for the analysis of various processes that deal with fluids, and in the case of heat exchangers it is widespread and has proven to be a reliable tool for analysis. An example is the study by Z.C. Liu and W. Liu. about the geometry of the pipes used in heat exchangers of shell and tube type, which has been shown to modifying the geometry of the tube and modifying the fluid flow patterns, which results in variations in heat transfer as well as the various flow regimes, and that as the fluid velocity increases thereby increasing the turbulence the heat transfer also increases [1].

The study of the loss of efficiency in heat exchangers because of corrosion or malfunction of the system is also important, as presented in the work of Torres-Tamayo et al., which explains how it affects resource consumption; in this work the coefficients of heat transfer by convection are determined as well as the impact of this corrosion decreased the system efficiency because it showed a decrease in the thermal efficiency of 70% in heat exchangers due to such problems [2, 3].

1.1. Experimental heat exchanger

The experimental heat exchanger is of tubular type, cross flow occurs at 90°, it comprises vertical tubes placed in a 10 × 4 matrix in an arrangement of square type [4] as shown in **Figure 1**.
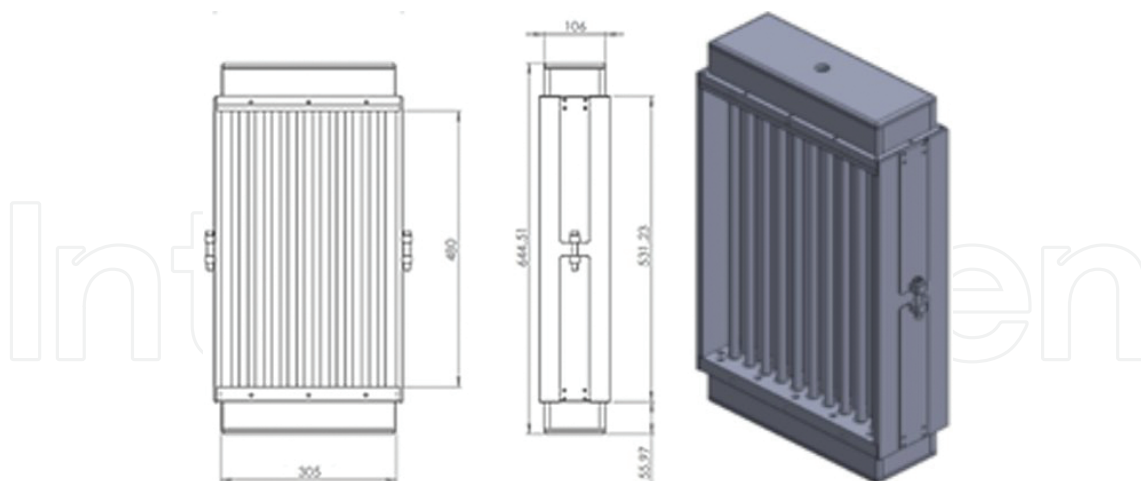

Figure 1. Frontal, lateral, and isometric view from heat exchanger (dimension in millimeters).

The heat exchanger is provided with an acrylic duct that is used to conduct the air to the tube arrangement (**Figure 2**). Water flows through 40 tubes vertically and constantly by means of a recirculation circuit which comprises a pump and a reservoir, and the air is supplied by a vertical fan.
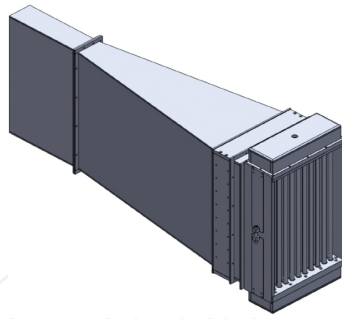
Figure 2. Isometric view of air duct and heat exchanger.

1.2. Instrumentation

The experimental heat exchanger is implemented with 32 fixed thermocouples, a flow meter is used to measure the flow of water, and readings of air velocity are taken during the test with an anemometer. Thirty-two thermocouples are connected to a data acquisition system in which the analogic signals received are changed to digital signals and then processed and captured in a computer using the LAB-VIEW software. In **Figure 3**, a diagram of the device with basic instrumentation installed therein to monitor the variables of interest is shown.
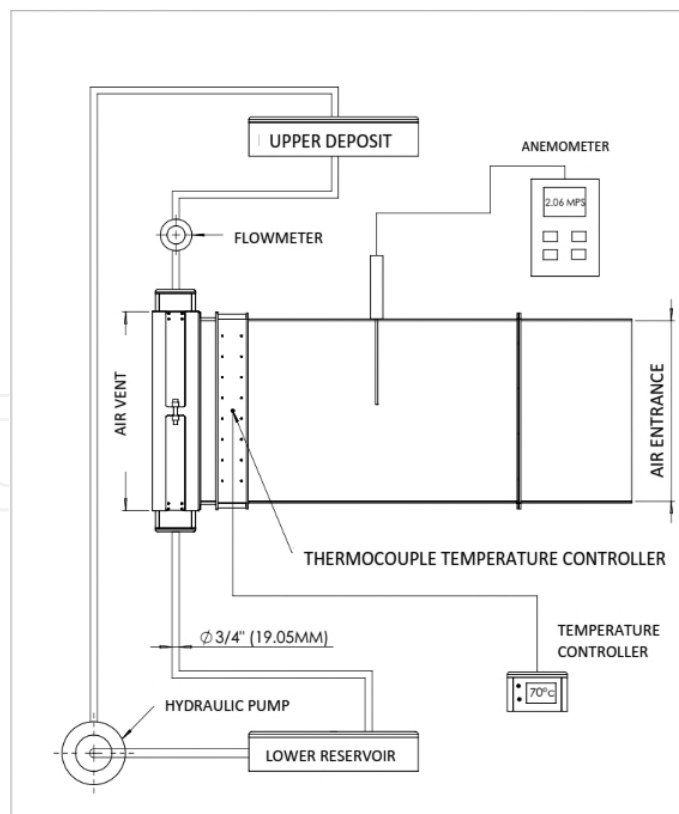

Figure 3. Diagram of instrumentation.

An anemometer was used to measure the velocity of the air entering to feed channel to heat exchanger (**Figure 4**).

Figure 4. Hot-wired anemometer.

A flowmeter is installed in the water supply pipe before entering into the arrangement of heat exchanger tubes (**Figure 5**).

Figure 5. Turbine flow meter installed in the water supply pipe.

The procedure for data collection is as follows:

1.   Ingress of air.

2.   Ingress of water (just to fill pipes).

3. Resistances are turned on for heating the air.

4. Temperatures are expected to stabilize and begin to measure air velocity in anemometer.

5. Water circulation starts and flow meter readings are taken.

6. Once the desired output and inlet temperatures on heat exchanger are achieved, about 15 min of data are taken.

Temperatures		
Water		
Variable	°C	K
T inlet	18.8000	291.9500
Inner wall (calculated)	28.9000	302.1500
T outlet	20.1600	293.3100
Air		
T inlet	63.1600	336.3100
T outer wall (action)	29.0000	302.1500
T outlet	32.8900	306.0400
Operation data		
Water flow rate	1.99×10^{-04}	m³/s
Air speed	1.2835	m/s

Table 1. Averaged variables from experimental measurements.

Water properties at 19°C (average)		
Density	998.8800	kg/m³
Cp	4184.4000	J/kg K
K	0.5962	W/m K
Viscosity	1.11×10^{-03}	kg/m s
Pr	7.8740	
Air properties at 48°C (average)		
Density	1.0970	kg/m³
Cp	1007	J/kg K
K	0.0272	W/m K
Viscosity	1.95×10^{-05}	kg/m s
Pr	0.7233	

Table 2. Averaged properties of fluids.

On the completion of the measurements and obtaining the data needed, these are organized and averages are computed, which are used for numerical simulation. The averages of the main variables measured are presented in **Table 1**. With the acquired data and obtaining the properties of both fluids, it is possible to calculate the rate of heat transfer and convective coefficients, and then they are used to perform numerical simulation. It is also necessary to calculate the average of fluid properties (**Table 2**).

1.3. Theoretical approach

The aim of the presented calculations is to obtain heat transfer and convective coefficients for both fluids. In reality, the convection phenomenon is complex and a constant numerical value for the heat convective coefficient is obtained; while stationary the heat transfer phenomenon is impossible; however, it is possible to obtain a representative average performing theoretical assumptions that are valid; in this case, the variables will be obtained with a theoretical model in which the same amount of heat is transferred with constant convective coefficients per unit average value area along the entire contact surface for both fluids [5]. The nomenclature of variables used on analytical calculation can be found in **Table 3**.

Variable	Symbol	Units
Density	ρ	kg/m^3
Specific heat	Cp	J/kg K
Thermal conductivity coefficient	k	W/m K
Dynamic viscosity	μ	kg/m s
Prandtl number	Pr	–
Temperature	T	K
Heat transfer	Q	W
Velocity	v	m/s
Volumetric flow	$\dot{v}$	m^3/s
Mass flow	$\dot{m}$	kg/s
Temperature gradient	ΔT	K
Convective coefficient	h	W/m^2 K
Nusselt number	Nu	–
Reynolds number	Re	–
Transversal section area	A_{ST}	m^2
Heat transfer area	A_{TC}	m^2
Inner diameter	D_i	m

Variable	Symbol	Units
Outer diameter	D_e	m
Diagonal passage	S_D	m
Longitudinal passage	S_L	m
Transversal passage	S_T	m
Thickness	l	m
Hydrodynamic inlet length	L_H	m
Thermal inlet length	L_T	m

Table 3. Nomenclature.

Subindex 1: Property or variable belonging to air.

Subindex 2: Property or variable belonging to water.

From equation for energy balance:

$$Q = \dot{m}_2 Cp_2 \Delta T_{2\,balance} \tag{1}$$

The total water mass flow:

$$\dot{m}_2 = \acute{v}_2\, \rho_2 \tag{2}$$

The temperature gradient for the energy balance is:

$$\Delta T_{2\,balance} = T_{2\,outlet} - T_{2\,inlet} \tag{3}$$

As the heat transfer rate is known, the heat transfer coefficient can be obtained from:

$$Q_{2\,conv} = h_2 A_{T2} \left(\Delta T_{C2} \right) \tag{4}$$

ΔT_{C2} can be obtained from:

$$\Delta T_{C2} = T_{inner\,wall} - T_{water\,average}$$

where

$$T_{water\ average} = \frac{T_{2\ outlet} + T_{2\ inlet}}{2}$$

the temperature of the inner wall is not known; however, the temperature of the outer wall, the tube thickness 1 mm, and thermal conductivity of copper tube, which is 380 W/m K and also has 40 tubes, are known; and as $Q_{cond} = Q_{convection} = Q_2$ it follows that:

$$T_{innerwall} = T_{outterwall} - \frac{\left(\frac{1}{40}\right)(Q_{conduction})\ln\left(\frac{r_{outter}}{r_{inner}}\right)}{2\pi L k} \tag{5}$$

As the temperature of the inner wall and the average water temperature are known, it is possible to obtain the heat transfer coefficient, which from Eq. (4) yields

$$h_2 = \frac{Q_{2\ convection}}{A_{T2}\left(\Delta T_{2C}\right)}$$

Now we can calculate the energy balance for air. First, the volumetric flow must be obtained:

$$\acute{v}_1 = v_1 A_{st1} \tag{6}$$

The air mass flow is calculated with the following equation:

$$\dot{m}_1 = \acute{v}_1 \rho_1 \tag{7}$$

Then, $Q_2 = Q_1$ and it is possible to obtain the heat transfer coefficient of air, using h from Eq. (4):

$$h_1 = \frac{Q_2}{A_{1T}\left(\Delta T_{1C}\right)}$$

The area for convection transfer to the air is

$$A_{T1} = 40\pi D_o L$$

And the temperature gradient ΔT_{1C} would be

$$\Delta T_{1C} = T_{airaverage} - T_{outterwall}$$

As the temperature of the outer wall is known, the average temperature is obtained as follows:

$$T_{(average\ air)} = \frac{\left(T_{(inletair)} + T_{(outletair)} \right)}{2}$$

All the above calculations are based on energy balances, but it is possible based on Nusselt numbers for comparison calculations. To calculate the Nusselt number for water, first obtain the Reynolds number to determine the conditions of the fluid:

$$Re_2 = \frac{\rho_2 v_2 D_i}{\mu_2} \tag{8}$$

The water velocity is given by

$$v_2 = \frac{\acute{v}_2}{A_{st2}} \tag{9}$$

The area $A_{ST\ 1}$ of the cross section for the flow of water is

$$A_{st2} = 40 \left(\frac{\pi D_o^{\,2}}{4} \right)$$

The Reynolds number describes the flow rate of fluids according to their size, and flow in a tube is considered laminar if it holds that $Re < 2300$. It is considered in transition if $2300 < Re < 4000$. And it is considered turbulent if $Re > 4000$ [5, 6].

The Nusselt number for a constant flow of heat per unit area for a fully developed flow and laminar flow along a circular pipe is 4.36. In this case, the water has a laminar flow and therefore the Nusselt number for this fluid is already known.

The heat transfer coefficient would be described by the following equation:

$$h_2 = \frac{Nu_2 k_2}{D_i} \tag{10}$$

And the heat transfer is obtained from Eq. (4):

$$Q_{2\,conv} = h_2 A_{T2}\left(\Delta T_{C2}\right)$$

where

$$A_{T2} = 40\pi D_i L$$

Now the mass coefficient is calculated based on the Nusselt number for air leaving the heat transferred by air which is absorbed by water $Q_2=Q_1$.

It is necessary to know the hydraulic diameter of the cross section that crosses in air:

$$D_h = L_c = \frac{4A_C}{P} \tag{11}$$

As the air flows through the matrix or tube bank, the speed will remain unchanged because the volume of air flow will be lower in the area where this is in contact with the tubes, and to maintain flow mass, the speed increases accordingly. Then, it is interesting to know the maximum speed reached by the air; this is the type of arrangement of the tube bank, and this case is rectangular arrangement type and the equation for the maximum speed is defined as

$$v_{max} = v\frac{S_T}{S_T - D_o} \tag{12}$$

And the Reynolds number according to Eq. (8) is

$$Re_2 = \frac{\rho v_{max} L_c}{\mu} \tag{13}$$

If the Reynolds number is the turbulent regime as in this case, the equation determined by Churchill and Bernstein can be applied, which is valid for all Reynolds numbers [6]:

$$Nu_1 = \frac{hD_o}{k} = 0.3 + \frac{0.62Re^{1/2}Pr^{1/3}}{\left(1+\left(\frac{0.4}{Pr}\right)^{2/3}\right)^{1/4}}\left(1+\left(\frac{Re}{282,000}\right)^{5/8}\right)^{4/5} \tag{14}$$

As the thermal conductivity of air is known from Eq. (10), it is possible to know the mass coefficient:

$$h_1 = \frac{Nu_1 k_1}{D_o}$$

2. Numerical simulation

The geometry used for the analysis has exactly the same dimensions as that of the heat exchanger installed on the laboratory (1:1 scale) in order to obtain data and represent both volumes of fluid (water and air) within the domain. This geometry was formed using the Solid Works software. Once completed, it is exported to the ICEM CFD software that is used to discretize the domain and to assign the name of the frontiers or boundaries of the total domain.

The discretization of the model is the partition or geometry in small elements called control volumes, where the Navier-Stokes equations will be evaluated, which govern fluid dynamics. For discretization, it is necessary to define the existing volumetric bodies; in this case, there are total 41 bodies; 40 of them are tubes, which represent the total volume of water, and the remaining body represents the air passing through them.

The discretization or (or mesh) selected was unstructured. Then, the parameters for the partition of the total volume into smaller volumes are set; these parameters are set in order to have the maximum size and the minimum size that can have the volume or item in a specific area.

Once meshed, the next step is to establish the boundary conditions in the domain; these conditions are very important because the solution is based on them and must be known before carrying out numerical simulation as these represent the actual phenomenon being simulated; and if they are not representative, it is impossible to validate such a simulation.

2.1. Preprocessing

For numerical simulation, the software ANSYS CFX was used, which is generally used to provide the numerical solution of differential equations of fluid dynamics. For solving such equations, the first step is known as preprocessing; at this stage, the discrete model is loaded and disclosed to the program boundary conditions, and to the parameters for the convergence of the solution. It was decided to separate the model into two domains as there are two fluids: one represents the total volume of water and the other the total volume of air as well as the respective boundaries. The boundary conditions are presented in **Table 4**.

2.2. Processing

At this stage, the Navier-Stokes equations are solved for each subdomain global system of equations.

1. The partial differential equations are integrated into all generated control volumes; the Navier-Stokes and models of thermal energy and turbulence are assigned to each node of each element or subdomain.

2. These integral equations become a global system of equations because each control volume is connected to the adjacent nodes.

3. The global system of equations is solved iteratively; this is necessary because of the nonlinear nature of the equations, and then the exact solution is approached for the solution. That is, the numerical solution obtained by each iteration should converge toward and approach a condition previously considered.

Zone	Boundary type	Condition	Variables	
External domain (turbulent air)			Magnitude	Temperature
Case	Wall	Adiabatic no slip	–	–
Air inlet	Inlet	Mass flow	$\dot{m} = 0.1284\,\text{kg}/\text{s}$	336.3100 K
Air outlet	Outlet	Pressure	0 Pa	306.0400 K
Outer tube wall	Wall	Convection No slip	$h_1 = 77.6200\,\text{W}/\text{m}^2\,\text{K}$	302.1500 K
Internal domain (laminar water)			Condition	Temperature
Water inlet	Inlet	Mass flow	$\dot{m} = 0.1987\,\text{kg/s}$	291.9500 K
Water outlet	Outlet	Pressure	0 Pa	293.3100 K
Inner tube wall	Wall	Convection no slip	$h_2 = 184.1873\,\text{W}/\text{m}^2\,\text{K}$	302.0400 K

Table 4. Boundary conditions for numerical simulation.

2.3. Postprocessing

Postprocessing is the final stage of CFD simulation, which allows visualizing the results of flow behavior inside the domain. There are several options to observe it, for example, contours, streamlines, and vectors. In the next section, the examples of post-processing are presented.

3. Results

As the results of the numerical simulation, fluids behave as expected according to the theory; for the case of water, as has flow within pipes, it is expected that the hydrodynamic and thermal layers are fully formed and have a length region input and a fully developed area.

As can be seen from **Figure 6**, tubes have an overall length sufficient for the water flow developing hydrodynamically and with a predominance of the fully developed flow as established in the calculations in Section 1.3.
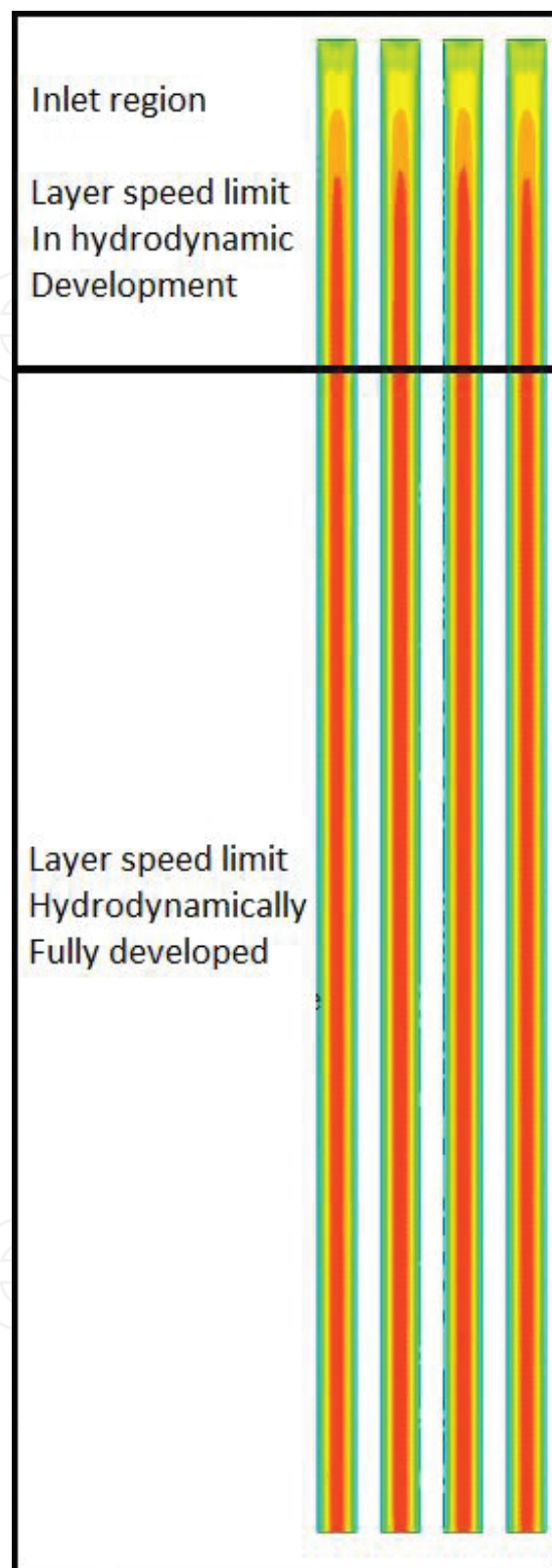
Inlet region

Layer speed limit
In hydrodynamic
Development

Layer speed limit
Hydrodynamically
Fully developed

Figure 6. Formation and development of the hydrodynamic boundary layer, velocity vectors in the inlet region, and development of the velocity boundary layer in the total length tubes.

The temperature of tubes wall is not constant for the thermal boundary layer, and, therefore, the thermal boundary layer has different temperatures at the interface of the tube wall and the fluid; as can be observed, it behaves correctly. **Figure 7** shows that the fluid cooler is located at the center of the tube, and the fluid is at a higher temperature at the boundary.

Theoretically, the air velocity should be higher where the circulating cross section (**Figure 8**) is reduced; wake vortices should also be formed, generated by the effect of separation of the hydrodynamic boundary layer in the tube wall (**Figure 9**).
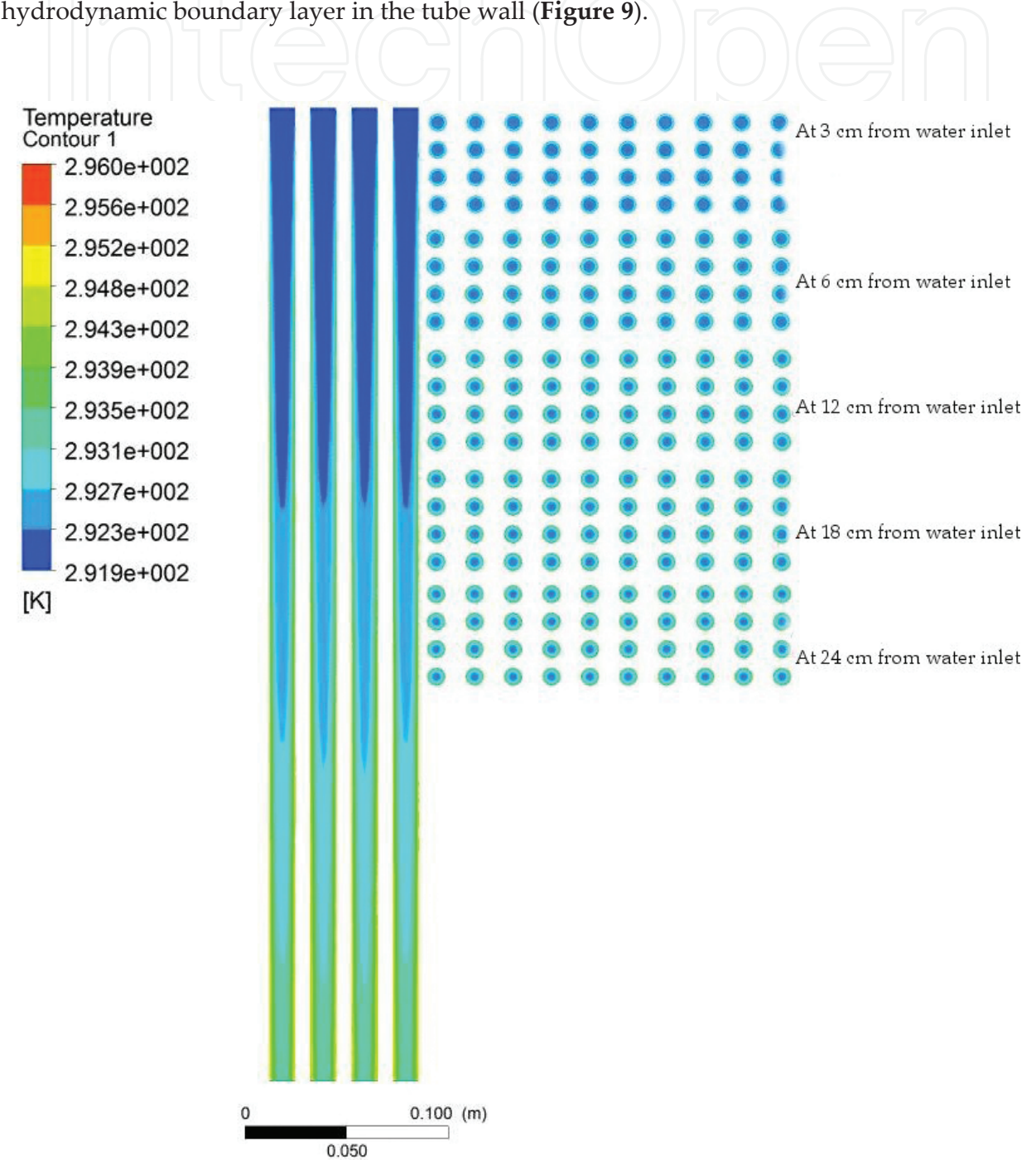
Figure 7. Development of thermal boundary layer: middle plane of tubes and transversal plane at different heights.
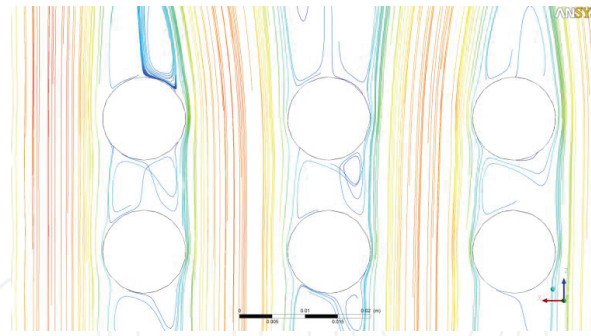
Figure 8. Air velocity contour in a cross section cut of 24 cm of the water inlet to the arrangement of pipes.
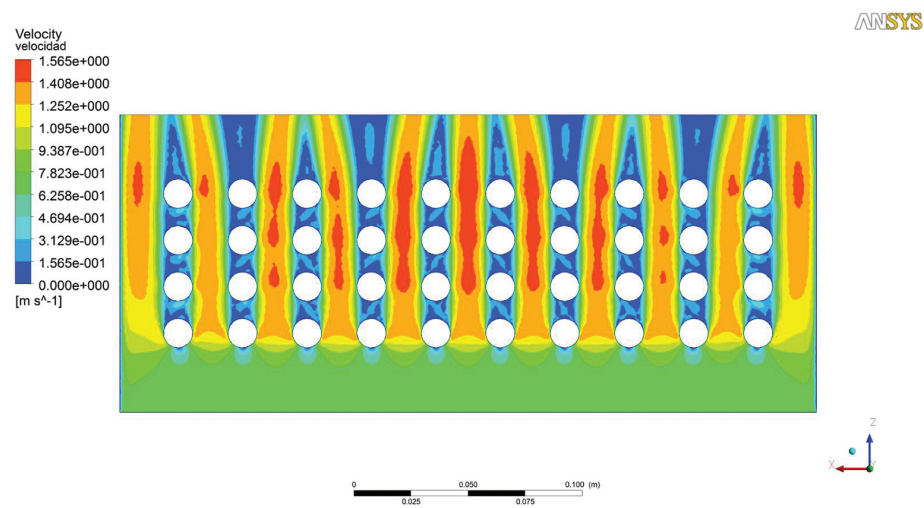

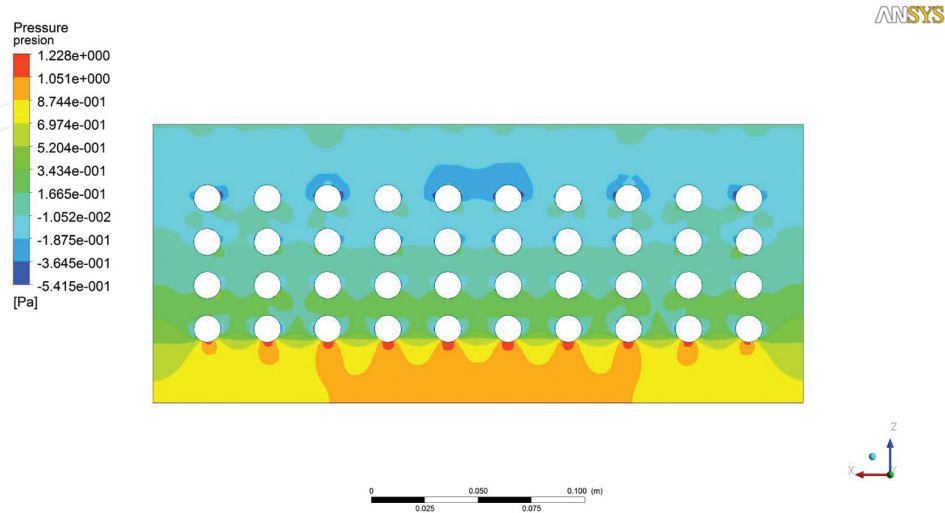**Figure 9.** Close-up view of streamlines of airflow at the transversal plane.

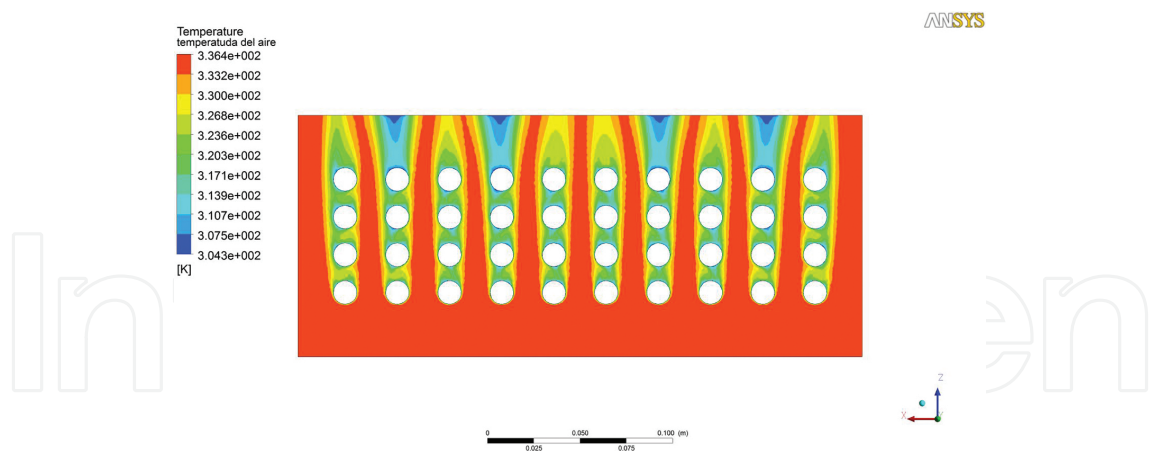**Figure 10.** Contour static gauge pressure in the matrix of tubes.

Figure 11. Outline temperature air flowing through the tube arrangement.

The maximum speed calculated theoretically was 1.711 m/s and from simulation it is 1.565 m/s, which represents a percentage error of 8.5% that can be considered small due to the complexity of the phenomenon. In the simulation results, it is possible to observe the formation of high-pressure areas where air directly enters the wall of the tube and low-pressure zones where the hydrodynamic wake zone (**Figure 10**) is generated.

For air temperatures, in a manner analogous to the water, the lower temperature is found at the boundary between the outer tube wall and the fluid as shown in **Figure 11**.

The average temperature difference in the tubes is approximately 4°C between numerical simulation and experimentally obtained (**Figure 12**) whereas the average temperature difference at the air outlet is about 6°C (**Figure 13**).
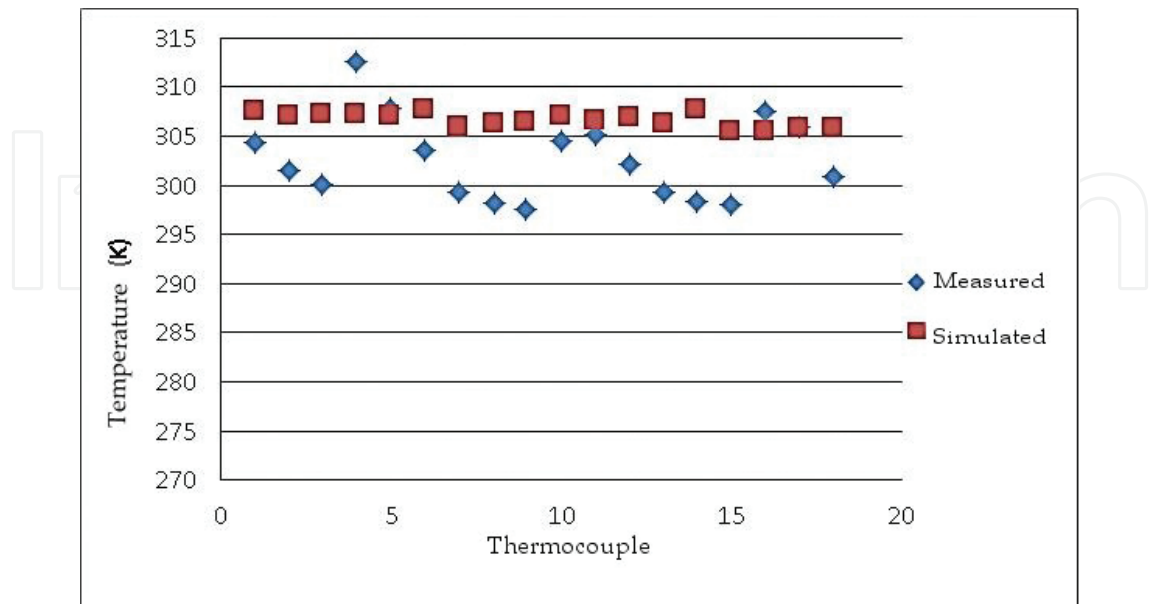

Figure 12. Temperatures measured vs. numerically simulated in the outer wall of tubes from the heat exchanger.
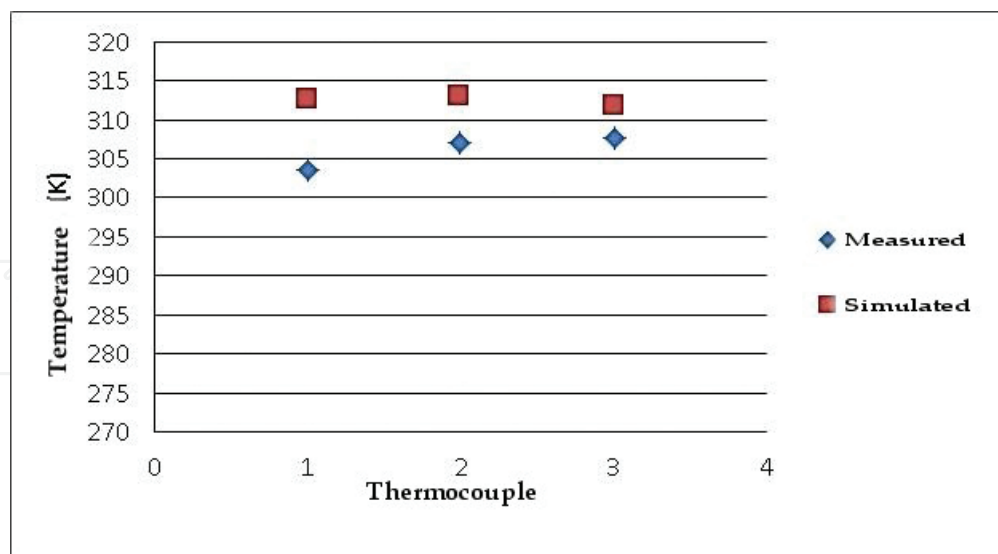
Figure 13. Temperatures measured vs. numerically simulated in the air outlet of the heat exchanger.

Although temperatures are not exactly the same, the differences are relatively small as well as the behavior is expected theoretically; it should also be noted that when working with heat transfer convection errors in physical quantities will usually be larger than with phenomena such as conduction, which is a complex phenomenon, as there are a greater number of variables involved.

Table 5 shows the results of calculus of heat transfer rate from both working fluids that are obtained by energy balances. In addition, the Nusselt number was calculated to subsequently obtain the convective coefficients of both fluids.

	Magnitude	Error
Q_{Water}	1131.1976 W	15.1500 %
Q_{air}	1333.1700 W	
Nu_{Water}	1489.5220 W	19.0130 %
Nu_{air}	1839.2200 W	

Table 5. Comparison of the magnitudes of the rate of heat transfer test analyzed.

In order to represent the efficiency of numerical simulations, the following ratio was calculated:

$$\eta = \frac{Q_{Real}}{Q_{Simulation}} = \frac{1131.19}{1333.17} = 0.85$$

which is quite acceptable for such heat transfer problems.

4. Conclusion

Numerical simulations were performed using different operational parameters for various measurements with experimental data in order to have a comprehensive approach to the analysis and comparison of experimental and simulated data.

The results of the numerical simulations were validated with calculations and the data obtained by measurements on the heat exchanger, with the average errors of 19% and 15%, respectively, for heat transfer calculus, considering that the phenomenon of convection is difficult to simulate perfectly because the equations and assumptions made to be represented analytically are not accurate enough.

Theoretically, the behavior of fluids and heat transfer was as expected. That is, it was possible to find out the results of the simulation of all phenomena involved in the convection generation of hydrodynamic and thermal boundary layers, the wake regions and production of vortices, and the areas of high and low pressures.

Author details

Laura L. Castro[*], Alfredo Aranda and Gustavo Urquiza

*Address all correspondence to: lauracg@uaem.mx

Research Center on Engineering and Applied Science (CIICAp), from the Autonomous University of Morelos State (UAEM), Morelos, Mexico

References

[1] Z.C. Liu, W. Liu.. 3D numerical study on shell side heat transfer and flow characteristics of rod-baffle heat exchangers with spirally corrugated tubes. International Journal of Thermal Sciences.. 2015;(89):34–42. DOI: doi:10.1016/j.ijthermalsci.2014.10.011

[2] Enrique Torres-Tamayo, Luís E. Quintana-Charlot, Orlando Vega-Arias, Yoalbys Retirado-Mediaceja. Coeficientes de transferencia de calor y pérdida de eficiencia en intercambiadores de calor de placas durante el enfriamiento del licor amoniacal. Minería y Geología. 2011;27(2):67–83.

[3] Agnieszka Flaga-Maryanczyk, Jacek Schnotale, Jan Radon, Krzysztof Was. Experimental measurements and CFD simulation of a ground source heat exchanger operating at a cold climate for a passive house ventilation system. Energy and Buildings. 2014;(68): 562–570. DOI: doi:10.1016/j.enbuild.2013.09.008

[4] Erick Omar Castañeda Magadán. Simulación Numérica y Construcción de un Intercambiador de Calor Experimental [[thesis]. Universidad Autónoma del Estado de Morelos:2015. 145 pp.

[5] Yunus A. Cengel, Afshin J. Ghajar. Heat and Mass Transfer. 4th ed. McGraw-Hill, USA; 2011. 921 pp.

[6] KakaÇ or Kakac, H. Liu. Heat Exchangers: Selection Rating and Thermal Design. 2nd ed. CRC, USA; 2002.